

# Stellar Evolution of Compact Stars in Curvature-Matter Coupling Gravity

M. Sharif <sup>\*</sup> and Arfa Waseem <sup>†</sup>

Department of Mathematics, University of the Punjab,  
Quaid-e-Azam Campus, Lahore-54590, Pakistan.

## Abstract

This paper is devoted to study the stellar evolution of compact objects whose energy density and pressure of the fluid are interlinked by means of MIT bag model and a realistic polytropic equation of state in the scenario of  $f(R, T, Q)$  gravity, where  $Q = R_{ab}T^{ab}$ . We derive the field equations as well as the hydrostatic equilibrium equation and analyze their solutions numerically for  $R + \delta Q$  functional form with  $\delta$  being a coupling parameter. We discuss the dependence of various physical properties such as pressure, energy density, total mass and surface redshift on the chosen values of the model parameter. The physical acceptability of the proposed model is examined by checking the validity of energy conditions, causality condition, and adiabatic index. We also study the effects arising due to matter-curvature coupling on the compact stellar system. It is found that maximum mass point lies within the observational range which indicates that our model is appropriate to describe dense stellar objects.

**Keywords:**  $f(R, T, Q)$  gravity; Compact stars; Equation of state.

**PACS:** 04.50.Kd; 04.40.Dg.

---

<sup>\*</sup>msharif.math@pu.edu.pk

<sup>†</sup>arfawaseem.pu@gmail.com

# 1 Introduction

Gravitational collapse is a fascinating phenomenon, responsible to produce remnants of massive stars known as compact objects. Compact objects are characterized by black holes, neutron stars and white dwarfs depending upon the mass of stellar objects. The final consequence of gravitational collapse entirely depends upon the original mass of the celestial bodies. Stars having a mass less than 8 solar mass ( $M_{\odot}$ ) construct white dwarfs whereas the stars possessing larger mass, transform into neutron stars or black holes as a result of the collapse. The existence of white dwarfs as well as neutron stars can be detected in our universe but the presence of black holes is affirmed only through some hypothetical observations.

The compact relativistic objects are extremely dense as well as relatively small whose pair can combine together to generate gravitational waves. Hawking [1] observed an upper limit for the gravitational radioactive energy ejected as a result of concussion between black holes. Wagoner [2] examined the energy produced by the rotation of neutron stars. In a region of higher gravitational potential, the observed electromagnetic radiations are redshifted in frequency and this phenomenon is referred as surface redshift ( $z_s$ ) which describes the relation between the interior geometry of star and its equation of state (EoS). The maximum bound for the surface redshift corresponding to isotropic as well as anisotropic spherical configurations are obtained as  $z_s \leq 2$  [3] and  $2 \leq z_s \leq 5$  [4], respectively. Böhmer and Harko [5] estimated the lower and upper limits of some viable constituents in the context of anisotropic fluid configuration with cosmological constant ( $\Lambda$ ). They found total energy bounds as well as redshift in terms of the anisotropic factor.

It is well-known that modified theories of gravity help to understand the current rapid expansion of cosmos. Such theories are formulated by the modification of gravitational part in Einstein-Hilbert action. The  $f(R)$  gravity [6] is the most smooth modified form of general relativity (GR) proposed by considering a generic form  $f(R)$  instead of Ricci scalar in the action of GR. Harko et al. [7] developed  $f(R, T)$  gravity by including the matter effects in  $f(R)$  theory, where T reveals the trace component of the stress tensor. The coupling between matter and gravitational parts yields a basic term which can produce fruitful results. It may provide a matter based deviation from the equation of motion and also assists to analyze dark source effects as well as late-time acceleration. Motivated by this argument, a more complicated

and extended theory having strong non-minimal curvature-matter combination is developed called  $f(R, T, Q)$  gravity [8, 9].

It is observed that theories similar to  $f(R, T)$  gravity are not the most general Lagrangians describing the non-minimal coupling between matter and geometry. An interesting difference in  $f(R, T)$  gravity and  $f(R, T, Q)$  gravity is that for  $T = 0$ , the  $f(R, T)$  field equations reduce to  $f(R)$  theory whereas in  $f(R, T, Q)$  gravity, the presence of  $Q$  still contains the strong effects of non-minimal coupling to the electromagnetic field. Sharif and Zubair [10, 11] checked the consistency of energy conditions in this theory and also discussed the validity of thermodynamical laws in the same scenario. Ayuso et al. [12] explored the physical viability and stability of this theory. Yousaf et al. [13] discussed the anisotropic stable structure of the cylindrical system as well as non-static spherical stellar models. In the same theory, Sharif and Waseem [14] investigated the regions of stable Einstein universe with linear EoS by considering homogeneous and inhomogeneous linear perturbations.

Compact objects are expressed as the basic ingredients in the field of astrophysics and cosmology. The study of physical properties and stability of these stars captivated the attention of many researchers. Mak and Harko [15] presented exact analytical solutions using linear EoS which describe anisotropic static spherical quark matter configuration. The same authors [16] also analyzed physical parameters (mass and radius) to discuss the features of neutron stars in GR. Chaisi and Maharaj [17] studied the anisotropic distribution of compact stars with the limiting case of energy density  $\rho \propto r^{-2}$ . Hossein et al. [18] investigated the structure of stellar system along with variable  $\Lambda$  which acts as a competent candidate of dark energy. The power series solutions using barotropic and polytropic EoS for perfect fluid distribution are also examined to analyze the hydrostatic stability of dense stellar objects [19]. Sharif and Sadiq [20] discussed the electromagnetic effects on the stability of stars for two polytropic EoS using perturbations on matter variables.

In recent years, the stability of self-gravitating system has become a captivating subject in modified or alternative theories of gravity. Sharif and Yousaf [21] observed the viability of spherical stellar system through perturbation approach in  $f(R, T)$  theory. Abbas et al. [22] established the physical characteristics of particular strange quintessence star models in  $f(R)$  scenario. The stellar stable configuration of quark as well as polytropic stars are also studied in  $f(R, T)$  gravity [23]. The physical features of some specific star models for different fluid distributions are investigated in  $f(R, T, Q)$

gravity [24]. Deb et al. [25] presented spherically symmetric isotropic quark stars governed by the MIT bag model in  $f(R, T)$  theory. They examined several physical properties of quark stars and showed their behavior graphically. Sharif and Siddiqa [26] analyzed the stellar models described by two different cases of polytropic EoS with anisotropic distribution in  $f(R, T)$  background. Recently, we have discussed the behavior of anisotropic quark stars by considering MIT bag model in the same framework. We have also determined the graphical behavior of particular compact star candidates [27].

From an astrophysical point of view, the scenario of stellar system investigates how stellar solution satisfies some general physical requirements. This paper is therefore dedicated to examine the physical conduct as well as the stability of compact stars to determine the constraints for which the system of stellar equations is physically realistic in  $f(R, T, Q)$  gravity. The format of the paper is presented as follows. In the next section, we present basic formalism of  $f(R, T, Q)$  gravity while in section 3, we derive the equations for the stellar structure and construct the system of differential equations using two EoS. Section 4 explores physical attributes of considered compact stars while the stability of our stellar system is analyzed in section 5. In the final section, we discuss the obtained results.

## 2 Basic Formulation of $f(R, T, Q)$ Gravity

The construction of  $f(R, T, Q)$  gravity is developed on the strong basis of non-minimal coupling of matter content and geometry. The modified action of this gravity along with matter Lagrangian  $\mathcal{L}_m$  is given as [8]

$$A = \frac{1}{2\kappa^2} \int \sqrt{-g} (f(R, T, Q) + \mathcal{L}_m) d^4x, \quad (1)$$

where  $\kappa^2 (= 1)$  is coupling constant and  $g$  is the determinant of the metric tensor ( $g_{ab}$ ). The standard energy-momentum tensor whose matter action based only on  $g_{ab}$  is defined by [28]

$$T_{ab} = -\frac{2}{\sqrt{-g}} \frac{\delta(\sqrt{-g}\mathcal{L}_m)}{\delta g^{ab}} = g_{ab}\mathcal{L}_m - \frac{2\partial\mathcal{L}_m}{\partial g^{ab}}. \quad (2)$$

The field equations are obtained by applying the variation on action (1) w.r.t  $g_{ab}$  as

$$R_{ab}f_R - \left( \frac{1}{2}f - \mathcal{L}_m f_T - \frac{1}{2}\nabla_\mu\nabla_\nu(f_Q T^{\mu\nu}) \right) g_{ab} + (g_{ab}\square - \nabla_a\nabla_b) f_R$$

$$\begin{aligned}
& + 2f_Q R_{\mu(a} T_{b)}^\mu - \nabla_\mu \nabla_{(a} [T_{b)}^\mu f_Q] + \frac{1}{2} \square (f_Q T_{ab}) + \frac{1}{2} R g_{ab} \mathcal{L}_m f_Q - R_{ab} \mathcal{L}_m f_Q \\
& - 2(f_T g^{\mu\nu} + f_Q R^{\mu\nu}) \frac{\partial^2 \mathcal{L}_m}{\partial g^{ab} \partial g^{\mu\nu}} = (1 + f_T + \frac{1}{2} R f_Q) T_{ab}, \tag{3}
\end{aligned}$$

where  $f_R \equiv \frac{\partial f}{\partial R}$ ,  $f_T \equiv \frac{\partial f}{\partial T}$  and  $\square \equiv \nabla^a \nabla_a$ . It is interesting to mention here that for vanishing  $Q$ , the field equations of  $f(R, T)$  theory can be regained which can be compressed further to obtain  $f(R)$  field equations for vacuum case. The covariant divergence of field equations (3) leads to

$$\begin{aligned}
\nabla^a T_{ab} &= \frac{2}{2(1 + f_T) + R f_Q} \left[ \nabla_a (f_Q R^{a\mu} T_{\mu b}) + \nabla_b (\mathcal{L}_m f_T) - G_{ab} \nabla^a (f_Q \mathcal{L}_m) \right. \\
&\quad \left. - \frac{1}{2} (f_Q R_{\mu\nu} + f_T g_{\mu\nu}) \nabla_b T^{\mu\nu} - \frac{1}{2} [\nabla^a (R f_Q) + 2 \nabla^a f_T] T_{ab} \right]. \tag{4}
\end{aligned}$$

It is quoted here that conservation equation does not hold in this modified theory similar to other theories of gravity having matter-curvature coupling [7]. The standard stress energy tensor for isotropic fluid distribution is

$$T_{ab} = (p + \rho) V_a V_b - p g_{ab}, \tag{5}$$

where  $p$  and  $\rho$  represent the pressure and energy density of the fluid, respectively and  $V_a = \sqrt{g_{00}}(1, 0, 0, 0)$  denotes four velocity in comoving coordinates which satisfies the condition  $V_a V^a = 1$ . For a perfect fluid, we have  $\mathcal{L}_m = -p$  that leads to  $\frac{\partial^2 \mathcal{L}_m}{\partial g^{ab} \partial g^{\mu\nu}} = 0$  [8].

Stellar evolution is a fascinating phenomenon because it is responsible for the construction of relativistic stellar objects. It is well-known that GR faces difficulties in explaining the universe at large scales beyond the solar system as well as at large energies. It seems natural to modify the Einstein gravity towards better understanding of gravity at a very large and very small scales. Since, the small modifications of GR may constitute an unstable system in the interior solution, a phenomenon referred to as matter instability. It is found that this instability can be removed by a convenient choice of the functional form of modified theories [9]. For a spherical stellar system, the modified field equations have to be solved both in the external as well as internal geometries of the celestial object. In the exterior, where  $T = 0$ , the field equations of  $f(R, T, Q)$  gravity reduce to the  $f(R)$  theory and their solutions behave as in GR. Nevertheless, interior solutions of the spherical system in  $f(R, T, Q)$  gravity may lead to large instabilities. This issue can

be resolved if we consider a viable model of this theory which satisfies the following conditions

$$3f_{RR} + \left(\frac{T}{2} - T^{00}\right) f_{QR} \geq 0, \quad \frac{1 + f_T + \frac{1}{2}Rf_Q}{f_R - f_Q\mathcal{L}_m} > 0.$$

The classification of functional forms regarding different configurations of matter in  $f(R, T, Q)$  gravity are presented as

$$f(R, T, Q) = \begin{cases} R + f(Q), \\ f_1(R) + f_2(Q), \\ f_1(R) + f_1(R)f_2(Q), \\ f_1(R) + f_2(T) + f_3(Q). \end{cases}$$

In this paper, we choose the first class, i.e.,  $f(R, T, Q) = R + f(Q)$  for which we consider  $f(Q) = \delta Q$  to study stable/unstable configurations of compact objects. This is the simplest functional form which describes the relation between geometry and matter only through the strong coupling between the Ricci and stress tensors. This model is first suggested by Haghani et al. [8] and has widely been used to study different cosmological issues. Haghani et al. [8] examined the evolution as well as dynamics of the universe corresponding to this model and found that for  $\delta > 0$ , this model well describes the expanding and collapsing phases of cosmos. The energy conditions as well as laws of thermodynamics are analyzed in this model. Baffou et al. [29] observed the stability of power law and de Sitter solutions for this model and found that the higher derivatives present in this theory can explore a new aspect regarding early phases of cosmic evolution. The physical features of compact stars using Krori-Barua solution have also been studied for this model [24]. Substituting this model along with  $\mathcal{L}_m = -p$  in Eq.(3), it follows that

$$\begin{aligned} G_{ab} &= \frac{1}{1 + \delta p} \left[ T_{ab} + \frac{\delta}{2} R T_{ab} + \frac{\delta}{2} \{ Q g_{ab} - \square T_{ab} - \nabla_\mu \nabla_\nu (T^{\mu\nu}) g_{ab} \} \right. \\ &\quad \left. - 2\delta R_{\mu(a} T_{b)}^\mu + \delta \nabla_\mu \nabla_{(a} T_{b)}^\mu \right], \end{aligned} \quad (6)$$

where  $G_{ab}$  is the usual Einstein tensor. Also, for the considered model, the non-conservation equation of the stress-energy tensor reduces to

$$\nabla^a T_{ab} = \frac{2\delta}{2 + \delta R} \left[ \nabla_a (R^{a\mu} T_{\mu b}) + G_{ab} \nabla^a (p) - \frac{1}{2} (R_{\mu\nu}) \nabla_b T^{\mu\nu} - \frac{1}{2} \nabla^a (R) T_{ab} \right]. \quad (7)$$

### 3 Equations of Stellar Structure

It is assumed that a star remains in a steady state described by static spherically symmetric metric given by

$$ds_-^2 = e^{\mu(r)} dt^2 - e^{\lambda(r)} dr^2 - r^2(d\theta^2 + \sin^2\theta d\phi^2). \quad (8)$$

For this interior geometry, the field equations (6) along with matter content (5) turn out to be

$$\begin{aligned} e^{-\lambda} \left( \frac{\lambda'}{r} - \frac{1}{r^2} \right) + \frac{1}{r^2} &= \frac{1}{1 + \delta p} \left[ \rho + \frac{\delta}{2} \left\{ \rho'' - p'' - \frac{2e^\lambda}{r^2} (\rho - p) + \left( \frac{4}{r} - \frac{\lambda'}{2} \right) \right. \right. \\ &\times (\rho' - p') + \rho \left( \mu'' + 2\mu'^2 - \mu'\lambda' + \frac{2}{r^2} - \frac{2\lambda'}{r} \right) + p \\ &\times \left. \left. \left( \frac{\mu''}{2} - \frac{\mu'}{r} - \frac{2}{r^2} - \frac{3\mu'\lambda'}{4} + \frac{2\lambda'}{r} + \frac{7\mu'^2}{4} \right) e^{-\lambda} \right\} \right], \quad (9) \\ e^{-\lambda} \left( \frac{\mu'}{r} + \frac{1}{r^2} \right) - \frac{1}{r^2} &= \frac{1}{1 + \delta p} \left[ p \left( 1 - \frac{\delta}{r^2} \right) + \frac{\delta e^{-\lambda}}{2} \left\{ \rho \left( \frac{\mu''}{2} + \frac{3\mu'^2}{4} + \frac{\mu'}{r} \right. \right. \right. \\ &+ \left. \left. \frac{\mu'\lambda'}{4} \right) + p \left( \frac{\mu'^2}{4} - \frac{\mu''}{2} + \frac{3\mu'}{r} - \frac{2}{r^2} + \frac{5\mu'\lambda'}{4} + \frac{2\lambda'}{r} \right. \right. \\ &\left. \left. \left. + \lambda'^2 + \lambda'' \right) + p' \left( \frac{\mu'}{2} + \frac{6}{r} + 2\lambda' \right) \right\} \right], \quad (10) \end{aligned}$$

where prime reveals derivative w.r.t radial coordinate. Moreover, from the non-conservation of the stress energy tensor (7), the hydrostatic equilibrium equation is calculated as

$$\begin{aligned} p' + (\rho + p) \frac{\mu'}{2} &= \frac{\delta}{2 + \delta R} \left[ 2p \left\{ \left( \frac{\mu'}{2} + \frac{2}{r} \right) \left( \frac{\lambda'}{r} + \frac{\mu'\lambda'}{4} - \frac{\mu'^2}{4} - \frac{\mu''}{2} \right) + \frac{\lambda''}{r} \right. \right. \\ &- \frac{\mu'''}{2} - \frac{\mu'\mu''}{2} + \frac{\mu'\lambda''}{4} + \frac{\mu''\lambda'}{2} + \frac{\mu'^2\lambda'}{8} - \frac{\lambda'}{r^2} + \frac{\mu'}{r^2} - \frac{\mu'\lambda'^2}{8} \\ &- \left. \left. \frac{\lambda'^2}{2r} + \frac{2}{r^3} \right\} + p e^\lambda \left\{ \frac{3\mu''\lambda'}{2} - \mu''' - \frac{4e^\lambda}{r^3} - \mu'\mu'' + \frac{\mu'^2\lambda'}{2} \right. \right. \\ &+ \left. \left. \frac{\mu'\lambda''}{2} - \frac{\mu'\lambda'^2}{2} + \frac{4\lambda'}{r^2} - \frac{2\lambda''}{r} + \frac{2\lambda'^2}{r} + \frac{2\mu'^2}{r} - \frac{2\mu''}{r} + \frac{2\mu'\lambda'}{r} \right\} \right. \\ &+ \left. \frac{2p'}{r^2} \left\{ e^\lambda(\mu'r - e^\lambda) + 1 - \frac{r\lambda'}{2} + \frac{\mu'r}{2} \right\} - (\rho' + \mu'\rho) \left( \frac{\mu''}{2} \right. \right. \end{aligned}$$

$$+ \left. \frac{\mu'}{r} - \frac{\mu'\lambda'}{4} + \frac{\mu'^2}{4} \right) \Big]. \quad (11)$$

It is interesting to note that field equations (9), (10) and conservation equation (11) reduce to standard GR equations [30, 31] for  $\delta = 0$ . From Eqs.(9)-(11), we obtain a set of three differential equations as

$$\begin{aligned} p'' &= p' \left( \frac{\lambda'}{2} - \frac{4}{r} \right) + p \left( \frac{\mu''}{2} - \frac{\mu'}{r} + \frac{7\mu'^2}{4} - \frac{3\mu'\lambda'}{4} + \frac{2e^\lambda}{r^2} \left( \frac{1-\delta}{\delta} \right) \right) + \rho'' \\ &+ \rho' \left( \frac{4}{r} - \frac{\lambda'}{2} \right) + \rho \left( 2e^\lambda \left( \frac{1}{\delta} - \frac{1}{r^2} \right) + \mu'' + 2\mu'^2 - \mu'\lambda' + \frac{2}{r^2} - \frac{2\lambda'}{r} \right), \end{aligned} \quad (12)$$

$$\begin{aligned} \lambda'' &= -\lambda' \left( \lambda' + \frac{2}{r} + \frac{2p'}{p} + \frac{4\mu'}{4} + \frac{\mu'\rho}{4p} \right) - \frac{2e^\lambda}{\delta} \left( \frac{1}{pr^2} + \frac{1}{\delta} \right) + 2 \left( \frac{1+\delta p}{\delta p} \right) \\ &\times \left( \frac{\mu'}{r} + \frac{1}{r^2} \right) - \frac{\rho}{p} \left( \frac{\mu''}{2} + \frac{\mu'}{r} + \frac{3\mu'^2}{4} \right) + \frac{\mu''}{2} - \frac{2}{r^2} - \frac{\mu'^2}{4} - \frac{3\mu'}{r} \\ &- \frac{p'}{p} \left( \frac{\mu'}{2} + \frac{6}{r} \right), \end{aligned} \quad (13)$$

$$\begin{aligned} \mu''' &= \frac{1}{1+e^\lambda} \left[ \mu'' \left\{ -e^{-\lambda} \left( \frac{p'}{p} + \frac{\mu'(\rho+p)}{2p} \right) - \frac{3\mu'}{2} - \frac{2}{r} + \lambda' + e^\lambda \left( \frac{3\lambda'}{2} - \mu' \right. \right. \right. \\ &- \left. \left. \frac{2}{r} \right) - \frac{\rho' + \mu'\rho}{2\delta p} \right\} + \mu' \left\{ e^{-\lambda} \left( \frac{p'}{p} \left( \frac{\lambda'}{2} - \frac{2}{r} - \frac{\mu'}{2} \right) + \frac{\mu'\lambda'}{4p} + (\rho+p) \right. \right. \\ &\times \left. \left. \left( \frac{\lambda'}{pr} - \frac{\mu'}{pr} - \frac{1}{pr^2} - \frac{\mu'^2}{4p} \right) \right) - \frac{\rho+p}{pr^2} + \frac{\mu'\lambda'}{2} + \frac{2\lambda'}{r} - \frac{\mu'^2}{4} - \frac{\mu'}{r} + \frac{\lambda''}{2} \right. \\ &+ \left. \frac{2}{r^2} - \frac{\lambda'^2}{4} + \frac{p'}{pr} + e^\lambda \left( \frac{\lambda''}{2} + \frac{\mu'\lambda'}{2} - \frac{\lambda'^2}{2} + \frac{2}{r^2} + \frac{2\lambda'}{r} + \frac{2p'}{pr^2} \right) \right\} \\ &- \left( \frac{\rho' + \mu'\rho}{\delta p} \right) \left( \frac{\mu'}{r} - \frac{\mu'\lambda'}{4} + \frac{\mu'^2}{4} \right) + \frac{2p'}{pr^2} \left( 2 - e^{2\lambda} - 2e^{-\lambda} - \frac{r\lambda'}{2} \right) \\ &+ \frac{2p'}{p} \left( \frac{\lambda'e^{-\lambda}}{r} - \frac{1}{\delta} \right) + e^\lambda \left( \frac{4\lambda'}{r^2} - \frac{2\lambda''}{r} + \frac{2\lambda'^2}{r} - \frac{4e^\lambda}{r^3} \right) \\ &+ \left. \frac{2\lambda'}{r^2} + \frac{2\lambda''}{r} + \frac{4}{r^3} - \frac{\lambda'^2}{r} \right]. \end{aligned} \quad (14)$$

Since we have a set consisting of three non-linear differential equations in four unknowns  $p$ ,  $\rho$ ,  $\lambda$  and  $\mu$ , so we need EoS which will be helpful to reduce one unknown parameter.

To solve the system of differential equations, we suppose a direct and systematic relation between pressure and density of the fluid which depicts the form of matter for the proposed set of physical constraints named as EoS. In compact stars, white dwarfs have masses about  $1.4M_{\odot}$  and their radii are much smaller than the sun. On the other hand, the neutron stars can possess larger masses up to  $3M_{\odot}$  [32]. The attractive gravitational effect in white dwarfs is dominated by the degeneracy pressure of electrons whereas in neutron stars, this balance is maintained by the degeneracy pressure of neutrons. Neutron stars are the utmost curious objects and can be further transformed into the black hole if they possess highly dense core whereas the slighter dense cores in neutron stars collapse into a quark star. The transition of quark stars from neutron stars has been discussed in literature [33]. The imaginary forms of compact objects formulated by three flavors (up, down and strange) are referred to as quark stars. The structure of these stars are smaller in size as well as highly dense and maintain an extreme gravitational field. In neutron stars as well as white dwarfs, pressure against the gravitational pull has the same source known as quantum pressure.

To define the polytropic stars, the polytropic EoS is given by

$$p = \alpha\rho^{1+\frac{1}{n}},$$

where  $n$  is a polytropic index and  $\alpha$  is a polytropic constant. In literature [34]-[36], it is found that the realistic EoS can be obtained through piecewise polytropic EoS with index  $n \in [0.5, 1]$ . To examine physical features of stellar models in  $f(R, T, Q)$  gravity, we consider MIT bag model given by the relation  $p = 1/3(\rho - 4\mathfrak{B})$ , where  $\mathfrak{B}$  symbolizes the bag constant (for quark stars) and realistic polytropic EoS  $p = \alpha\rho^2$  (corresponds to neutron stars). These EoS have been used successfully for the analysis of stellar configuration of compact stars [23, 26, 27, 34]-[36].

## 4 Physical Properties of Compact Stars

In this section, we analyze the physical consistency of stellar equations to observe the properties of compact stars. With the help of EoS, we solve the stellar structure equations numerically using initial conditions for different values of  $\delta$ . In the interior of stellar models, the density and pressure should be positive, finite as well as regular at all points. Applying this behavior

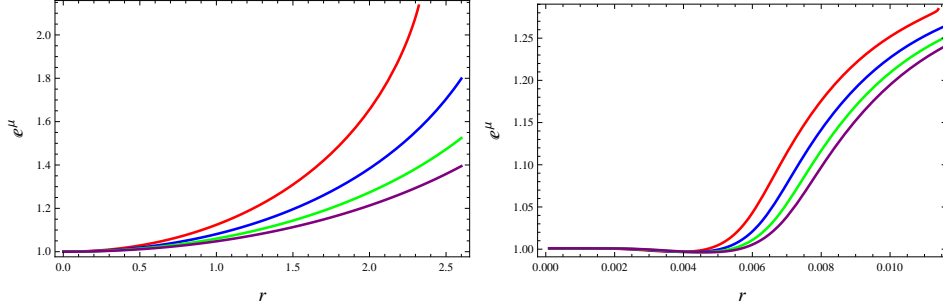


Figure 1: Variation of  $e^\mu$  versus  $r$  with MIT bag model (left) and polytropic EoS (right) for  $\delta = 2$  (red),  $\delta = 3$  (blue),  $\delta = 4$  (green) and  $\delta = 5$  (purple).

at the center  $r = 0$ , we obtain the following initial conditions from the field equations

$$\begin{aligned} \mu''(0) = 0, \quad \mu'(0) = 0, \quad \mu(0) = 0, \quad \lambda'(0) = 0, \\ \lambda(0) = 0, \quad p(0) = p_c, \quad \rho(0) = \rho_c, \quad p'(0) = 0, \end{aligned} \quad (15)$$

where  $\rho_c$  and  $p_c$  represent some central values which we fix for numerical analysis. Also, consideration of EoS decreases one condition such that we need only the value of  $p(0)$ . In this paper, we take  $\mathfrak{B} = 60 \text{ MeV}/\text{fm}^3$  [23],  $\alpha = 4.7802810^{-5} [\text{fm}^3/\text{MeV}]^{2/3}$  and  $p_c = 200 \text{ MeV}/\text{fm}^3$  [26]. Throughout this analysis, we are employing the units of mass as  $M_\odot$ , density (pressure) as  $\text{MeV}/\text{fm}^3$  and radius as  $km$  [23, 26].

#### 4.1 Metric Functions, Density and Pressure

Here, we examine the role of metric functions, energy density and pressure for both quark as well as polytropic compact stars for different values of  $\delta$ . The variation of physical parameters  $e^\mu$ ,  $e^\lambda$ ,  $p$  and  $\rho$  versus radial coordinate are featured in Figures 1-4. From Figure 1, it is observed that with the increasing value of  $\delta$ , the metric function  $e^\mu$  decreases for both MIT bag model and polytropic EoS. The graphical behavior of other metric function  $e^\lambda$  also reduces for both EoS with the increment in the model parameter  $\delta$  as shown in Figure 2. However, the behavior of these metric potentials is positive definite which shows that our set of stellar system vanishes any kind of singularity.

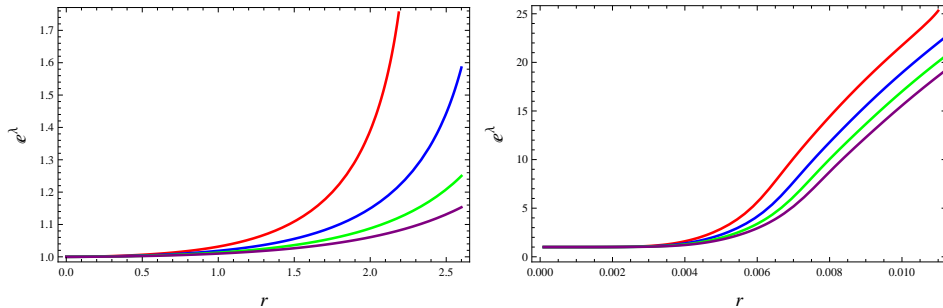


Figure 2: Variation of  $e^\lambda$  versus  $r$  with MIT bag model (left) and polytropic EoS (right) for  $\delta = 2$  (red),  $\delta = 3$  (blue),  $\delta = 4$  (green) and  $\delta = 5$  (purple).

In the interior of dense compact stars, the pressure as well as energy density should possess maximum value at the center. Figures 3 and 4 exhibit that these physical quantities have maximum behavior at  $r = 0$  and decrease towards the surface of compact objects. It is also observed that the values of these matter variables increase with increasing values of  $\delta$  which depicts the existence of dense cores of compact stars under the strong influence of coupling term  $Q$ . From the graphical analysis, it is found that the effect of pressure corresponding to quark stars is zero for  $\delta = 2$  at  $r \approx 2.33km$  whereas using realistic polytropic EoS, it vanishes at  $r \approx 0.014km$  for the same value of coupling parameter. It is worth mentioning here that the radius obtained for quark stars is physically viable while the radius observed for realistic polytropic EoS is much smaller than the predicted radii of neutron stars. However, in the context of  $f(R, T)$  gravity, the physical attributes of the stellar system with radius  $r \approx 0.06km$  have been discussed in literature for realistic polytropic EoS [37].

## 4.2 Energy Conditions

To examine the nature of normal or exotic matter in the interior geometry of compact objects, energy conditions play a vital role. The consistency of these conditions are governed by satisfying the following inequalities [38]

- NEC:  $\rho + p \geq 0$ ,
- SEC:  $\rho + p \geq 0, \quad \rho + 3p \geq 0$ ,
- DEC:  $\rho \geq 0, \quad \rho - p \geq 0$ ,

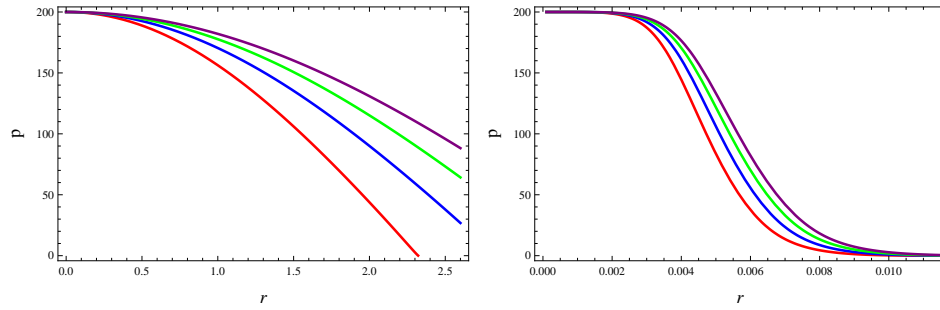


Figure 3: Plot of  $p$  versus  $r$  with MIT bag model (left) and polytropic EoS (right) for  $\delta = 2$  (red),  $\delta = 3$  (blue),  $\delta = 4$  (green) and  $\delta = 5$  (purple).

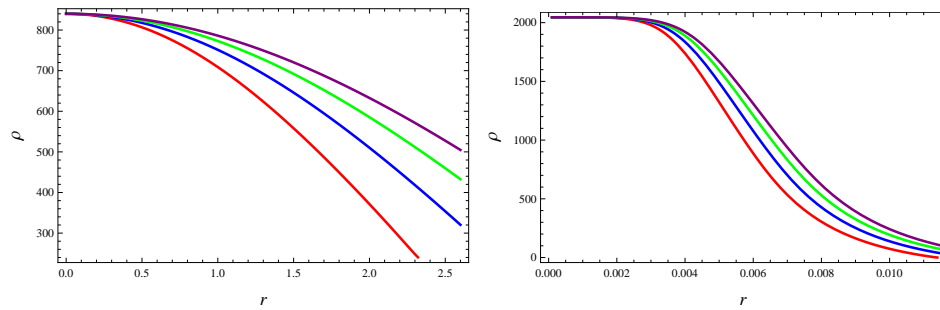


Figure 4: Plot of  $\rho$  versus  $r$  with MIT bag model (left) and polytropic EoS (right) for  $\delta = 2$  (red),  $\delta = 3$  (blue),  $\delta = 4$  (green) and  $\delta = 5$  (purple).

- WEC:  $\rho + p \geq 0, \quad \rho \geq 0.$

Figure 5 indicates that our system of differential equations, adopting two EoS, is feasible with all energy conditions for different values of  $\delta$  which also affirms the physical acceptability of particular functional form of this gravity.

### 4.3 Mass-Radius Relation and Surface Redshift

Here, we investigate mass as well as surface redshift of the compact stars for considered EoS with radial coordinate. At the boundary of the star's surface, i.e., at  $r = R$ , the interior solution of stellar objects connects smoothly with the Schwarzschild vacuum solution. The Schwarzschild approach has widely been used from different possibilities of the matching conditions to explore the features of stellar compact objects [39]. At the boundary ( $r = R$ ), the interior as well as exterior geometries are linked together by the following relation

$$e^{\lambda(R)} = \left(1 - \frac{2M}{R}\right)^{-1}, \quad (16)$$

where  $M$  reveals the total mass of stellar objects. The expression of  $M$  can be calculated from Eq.(16) as

$$M = \frac{R}{2} (1 - e^{-\lambda(R)}).$$

The surface redshift is also a significant phenomenon to interpret the dynamics of strong interaction between internal distribution of a star and its EoS. The formula for  $z_s$  corresponding to mass-function is defined as

$$z_s = \left(1 - \frac{2M}{R}\right)^{-1/2} - 1.$$

For static spherically symmetric configurations with perfect fluid distribution, the maximum bound for the surface redshift parameter is obtained as  $z_s \leq 2$  [3]. The graphical behavior of mass-radius relation as well as redshift parameter is presented in Figures 6 and 7. Figure 6 shows that the value of mass-function decreases with increasing values of  $\delta$ . In  $f(R, T)$  scenario, it is observed that the maximum mass  $2.17M_\odot$  and  $z_s \approx 0.4$  are obtained for MIT bag model [25]. In our case for  $\delta = 2$ , the maximum mass  $0.5M_\odot$  and  $0.006M_\odot$  are attained for quark and polytropic stars, respectively. It is also found that the bound of surface redshift is in good agreement with the required bound for both EoS as shown in Figure 7.

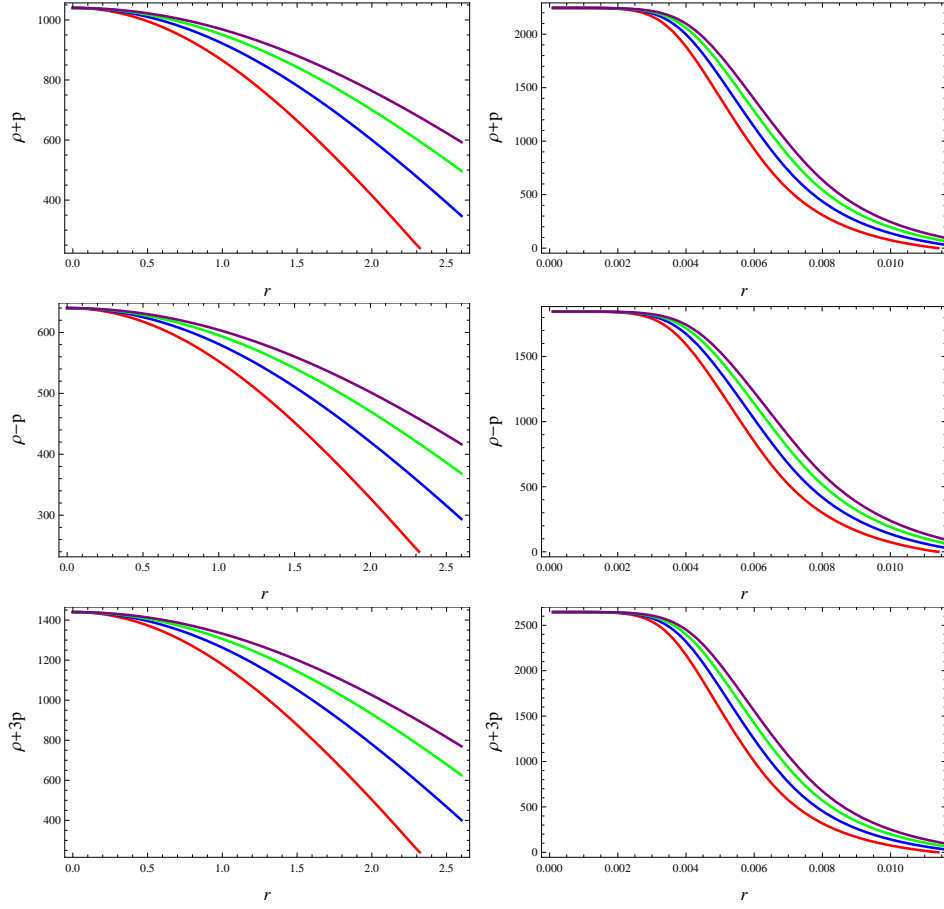


Figure 5: Behavior of energy conditions with MIT bag model (left) and polytropic EoS (right) for  $\delta = 2$  (red),  $\delta = 3$  (blue),  $\delta = 4$  (green) and  $\delta = 5$  (purple).

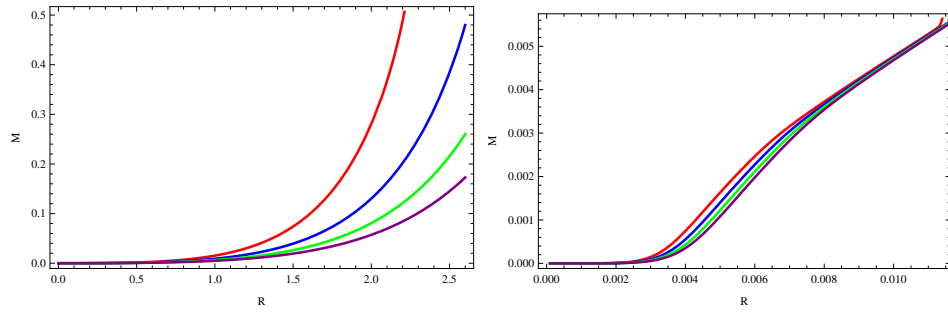


Figure 6: Mass-radius relation with MIT bag model (left) and Polytropic EoS (right) for  $\delta = 2$  (red),  $\delta = 3$  (blue),  $\delta = 4$  (green) and  $\delta = 5$  (purple).

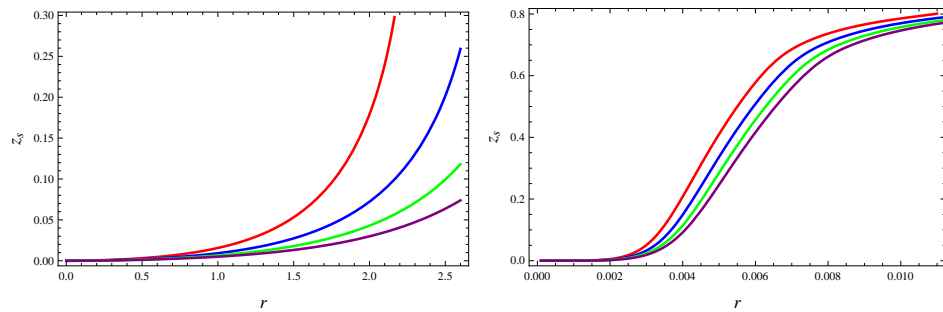


Figure 7: Plot of redshift versus  $r$  with MIT bag model (left) and Polytropic EoS (right) for  $\delta = 2$  (red),  $\delta = 3$  (blue),  $\delta = 4$  (green) and  $\delta = 5$  (purple).

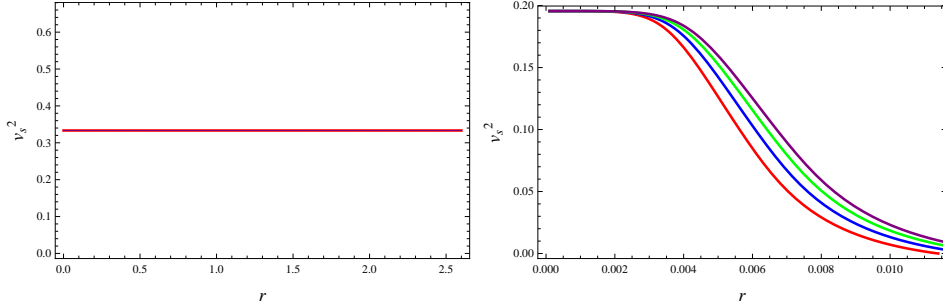


Figure 8: Behavior of speed of sound versus  $r$  with MIT bag model (left) and Polytropic EoS (right) for  $\delta = 2$  (red),  $\delta = 3$  (blue),  $\delta = 4$  (green) and  $\delta = 5$  (purple).

## 5 Stability of Compact Objects

The stability of relativistic structure has great importance in analyzing physically acceptable models. We investigate the stability of compact stars using two EoS by examining causality condition and adiabatic index.

### 5.1 Causality Condition

Here, we are interested to check the speed of sound ( $v_s^2$ ) using Herrera's cracking concept [40]. The causality condition demands that the squared sound speed represented by  $v_s^2 = dp/d\rho$  should be in the interval  $[0, 1]$ , i.e.,  $0 \leq v_s^2 \leq 1$  everywhere inside the stellar model for a physically acceptable object. Figure 8 reveals that for quark stars, we have a constant required value of  $v_s^2$  which is completely matched with the observed value of speed of sound in  $f(R, T)$  gravity [25] while for polytropic EoS, the value of speed of sound lies within the required range and it is also monotonically decreasing towards the surface of stars. Hence, our system of stellar equations is consistent with the required causality condition for both EoS and shows stable structure for all considered values of the coupling parameter.

### 5.2 Adiabatic Index ( $\Gamma$ )

The stiffness of the EoS corresponding to considered energy density is described by the adiabatic index which plays a major role to analyze the stability of stellar models. Chandrasekhar (as a pioneer) [41] and many researchers

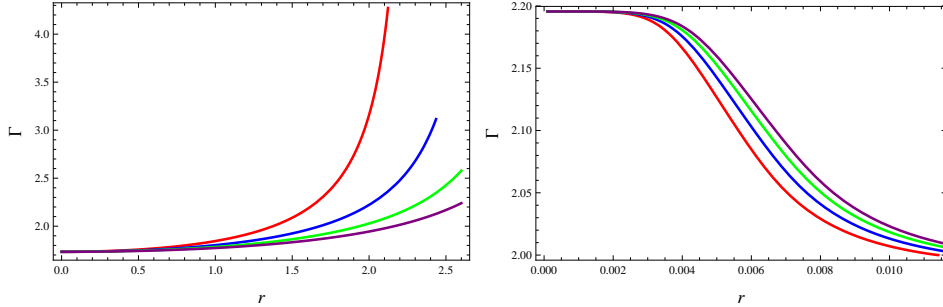


Figure 9: Plots of adiabatic index versus  $r$  with MIT bag model (left) and polytropic EoS (right) for  $\delta = 2$  (red),  $\delta = 3$  (blue),  $\delta = 4$  (green) and  $\delta = 5$  (purple).

[42] inspected the dynamical stability of the stellar system. It is predicted that the adiabatic index must be  $> \frac{4}{3}$  for a dynamically stable stellar object [42]. The expression for adiabatic index is of the form

$$\Gamma = \frac{\rho + p}{p} (dp/d\rho) = \frac{\rho + p}{p} (v_s^2).$$

The graphical interpretation of the adiabatic index is exhibited in Figure 9 for both EoS. This depicts that the set of stellar equations is dynamical stable for all values of the coupling parameter  $\delta$  as the values of  $\Gamma > \frac{4}{3}$  for both quark as well as realistic polytropic stars.

## 6 Discussion and Conclusions

This paper explores the physical attributes as well as dynamical stability of compact objects with two EoS (MIT bag model and realistic polytropic) in the framework of  $f(R, T, Q)$  gravity. The physical properties of proposed compact stars have been observed by deriving equations of stellar structure and hydrostatic equilibrium equation for  $R + \delta Q$  gravity model. The hydrostatic equilibrium equation, also known as Tolman-Oppenheimer-Volkoff (TOV) equation, is an extension due to the presence of extra terms coming from  $\delta Q$ . The stellar configurations of quark and polytropic stars have been analyzed for different values of the model parameter  $\delta$ .

We have constructed a system of differential equations and derived the initial conditions required for the numerical analysis. The variation of metric

functions (Figures 1 and 2) reveals that our system of stellar equations is free from any type of geometrical or physical singularity. The regularity conditions for energy density as well as pressure are also satisfied. It is found that at the center, stars exhibit maximum pressure and density which decrease monotonically towards the boundary of the stellar objects. The radii of approximately  $2.33km$  and  $0.014km$  are observed for quark and polytropic stars, respectively. In the background of gravity, it is investigated that the radius of realistic polytropic star is smaller than the inspected radius of neutron stars. Our stellar system is also found to be consistent with all energy bounds for all suggested values of  $\delta$  (Figure 5).

The mass-radius relation as well as surface gravitational redshift indicate that the maximum mass point for quark stars is  $0.5M_{\odot}$  while for polytropic stars is  $0.006M_{\odot}$  at  $\delta = 2$ . The maximum surface redshift are approximately equal to 0.3 and 0.8 for MIT bag model and polytropic EoS, respectively. The graphical analysis predicts that with the increment in the values of  $\delta$ , the mass of stars reduces and density in the interior of stars gradually increases which suggests the existence of utmost dense relativistic objects. We have obtained that the speed of sound for all values of  $\delta$  shows constant behavior inside the system for quark stars and lies between  $[0, 1]$  for both quark as well as polytropic stars which confirms that the stars for both EoS are stable. The behavior of adiabatic index in Figure 9 shows that  $\Gamma > \frac{4}{3}$  for both types of compact stars, which verifies the stability against an infinitesimal radial adiabatic perturbation.

In GR, there are some upper bounds on the masses of white dwarfs and neutron stars. According to Chandrasekhar [41], the maximum mass limit of a white dwarf is  $1.4M_{\odot}$  and the TOV limit [42] provides an upper limit of  $3M_{\odot}$  for neutron stars. In  $f(R, T)$  scenario, Moraes et al. [23] analyzed the features of compact objects and determined that the higher values of coupling parameter provide the structures of compact stars with larger masses. Astashenok et al. [43] investigated the properties of neutron and quark stars in  $f(R)$  gravity and found that positive values of the model parameter yields stable solutions, whereas the negative values lead to unstable stellar structures. They also observed that the values of masses decrease with the increasing values of the model parameter. In  $f(R, T)$  framework, Sharif and Siddiq [44] considered the MIT bag model and polytropic EoS to examine the nature of quark stars and white dwarfs, respectively. They observed that the masses of compact stars can cross the Chandrasekhar and TOV limits in the presence of higher-curvature terms.

It is worthwhile to mention here that the maximum values of masses obtained in  $f(R, T, Q)$  gravity lie very well within the required limits in GR and larger values of the model parameter  $\delta$  lead to the smaller masses of compact stars. It is also noticed that this gravity provides the existence of very small stellar objects as the radii obtained in this gravity are smaller than the radii observed in the above mentioned works.

### Acknowledgment

We would like to thank the Higher Education Commission, Islamabad, Pakistan for its financial support through the *Indigenous Ph.D. 5000 Fellowship Program Phase-II, Batch-III*.

## References

- [1] Hawking, S.W.: Phys. Rev. Lett. **26**(1971)1344.
- [2] Wagoner, R.V.: Astrophys. J. **278**(1984)345.
- [3] Buchdahl, H.A.: Phys. Rev. **116**(1959)1027.
- [4] Ivanov, B.V.: Phys. Rev. D **65**(2002)104011.
- [5] Böhmer, G. and Harko, T.: Class. Quantum Grav. **23**(2006)6479.
- [6] Capozziello, S.: Int. J. Mod. Phys. D **483**(2002)11; Nojiri, S. and Odintsov, S.D.: Phys. Rev. D **68**(2003)123512.
- [7] Harko, T. et al.: Phys. Rev. D **84**(2011)024020.
- [8] Haghani, Z. et al.: Phys. Rev. D **88**(2013)044023.
- [9] Odintsov, S.D. and Sáez-Gómez, D.: Phys. Lett. B **725**(2013)437.
- [10] Sharif, M. and Zubair, M.: J. High Energy Phys. **12**(2013)079.
- [11] Sharif, M. and Zubair, M.: J. Cosmol. Astropart. Phys. **11**(2013)042.
- [12] Ayuso, I., Jiménez, J.B. and Cruz-Dombriz, Á.: Phys. Rev. D **91**(2015)104003.

- [13] Yousaf, Z., Bhatti, M.Z. and Farwa, U.: *Class. Quantum Grav.* **34**(2017)145002; *Eur. Phys. J. C* **77**(2017)359.
- [14] Sharif, M. and Waseem, A.: *Mod. Phys. Lett. A* **33**(2018)1850216; *Eur. Phys. J. Plus* **133**(2018)160.
- [15] Mak, M.K. and Harko, T.: *Chin. J. Astron. Astrophys.* **2**(2002)248.
- [16] Mak, M.K. and Harko, T.: *Proc. Roy. Soc. Lond. A* **459**(2003)393.
- [17] Chaisi, M. and Maharaj, S.D.: *Pramana J. Phys.* **66**(2006)609.
- [18] Hossein, S.K.M. et al.: *Int. J. Mod. Phys. D* **21**(2012)1250088.
- [19] Harko, T. and Mak, M.K.: *Astrophys. Space Sci.* **361**(2016)283.
- [20] Sharif, M. and Sadiq, S.: *Eur. Phys. J. C* **76**(2016)568.
- [21] Sharif, M. and Yousaf, Z.: *Astrophys. Space Sci.* **354**(2014)471.
- [22] Abbas, G., Zubair, M. and Mustafa, G.: *Astrophys. Space Sci.* **358**(2015)26.
- [23] Moraes, P.H.R.S., José D.V.A. and Malheiro, M.: *J. Cosmol. Astropart. Phys.* **06**(2016)005.
- [24] Sharif, M. and Waseem, A.: *Eur. Phys. J. Plus* **131**(2016)190; *Can. J. Phys.* **94**(2016)1024.
- [25] Deb, D. et al.: *J. Cosmol. Astropart. Phys.* **03**(2018)044.
- [26] Sharif, M. and Siddiqa, A.: *Eur. Phys. J. Plus* **133**(2018)226.
- [27] Sharif, M. and Waseem, A.: *Eur. Phys. J. C* **78**(2018)868; *Int. J. Mod. Phys. D* **27**(2018)1950007; *ibid.* **28**(2019)1950033.
- [28] Landau, L.D. and Lifshitz, E.M.: *The Classical Theory of Fields* (Pergamon Press, 1971).
- [29] Baffou, E.H., Houndjo, M.J.S. and Tossa, J.: *Astrophys. Space Sci.* **361**(2016)1.
- [30] Tolman, R.C.: *Phys. Rev.* **55**(1939)364.

- [31] Openheimer, J.R. and Volkoff, G.M.: Phys. Rev. **55**(1939)374.
- [32] Shapiro, S.L. and Teukolsky, S.A.: *Black Holes, White Dwarfs and Neutron Stars The Physics of Compact Objects* (John Wiley and Sons, 1983).
- [33] Haensel, P., Zdunik, J.L. and Schaeffer, R.: Astron. Astrophys. **160**(1986)121; Glendenning, N.K.: Phys. Rev. D **46**(1992)1274; Lattimer, J. M. and Prakash, M.: Astrophys. J. **550**(2001)426.
- [34] Lattimer, J.M. and Prakash, M.: Astrophys. J. **550**(2001)426.
- [35] Lai, X.Y. and Xu, R.X.: Astropart. Phys. **31**(2009)128.
- [36] Yagi, K. and Yunes, N.: Phys. Rept. **681**(2017)1.
- [37] Sharif, M. and Siddiqa, A.: Eur. Phys. J. Plus **132**(2017)529.
- [38] Visser, M.: Phys. Rev. D **56**(1997)7578.
- [39] Regge, T. and Wheeler, J.A.: Phys. Rev. **108**(1957)1063.
- [40] Herrera, L. and Barreto, W.: Phys. Rev. D **88**(2013)084022.
- [41] Chandrasekhar, S.: Astrophys. J. **140**(1964)417.
- [42] Heintzmann, H. and Hillebrandt, W.: Astron. Astrophys. **38**(1975)51; Hillebrandt, W. and Steinmetz, K.O.: Astron. Astrophys. **53**(1976)283; Bombaci, I.: Astron. Astrophys. **305**(1996)871.
- [43] Astashenok, A.V., Odintsov, S.D. and de la Cruz-Dombriz, A.: Class. Quantum Grav. **34**(2017)205008.
- [44] Sharif, M. and Siddiqa, A.: Int. J. Mod. Phys. D **27**(2018)1850065.